geoconvention
Virtual Event September 21-23 2020
CSPG • CSEG • CWLS • GAC • MAC • IAH

Elastic depth trends for siliciclastic sequences

Lev Vernik and Jeremy Gallop
Ikon Science

Summary

Elastic and petrophysical depth trends are an integral component of reservoir characterization whether explicitly or implicitly constructed. Applications includes seismic inversion, pore pressure estimation and geostatistical model building. Typical workflows involve fitting well logs with smooth curves, without reference to known lithology specific templates that could provide realistic constraints. We examine clay-dependent porosity-depth trends for sandstones and shales in the context of *in situ* measurements from literature that reflect normal mechanical compaction. These porosity trends are then used as inputs to well-known rock physics models to provide median trends with bounds on elastic data as a function of depth. The elastic trends show good conformance to the available data and provide an important quality control for depth-trend analysis in all subsequent applications.

Method

We employ and modify known porosity-stress trends from the literature and then make use of rock physics relationships to link the porosities with formation P- and S- wave velocities, to constrain the acoustic and shear impedance trends and bounds for normally compacted sediments. To validate our models, we make comparisons with a data set comprised of mixed core and log measurements (Issler, 1992; Vernik, 2016). These data include total porosity and P-wave velocity in relatively homogeneous 5-10 m shale intervals limited to the 500-3500 m gross depth range. With a few exceptions, this range contains mostly normally compacted sediments with quasi-hydrostatic pore pressure.

Vertical effective stress is required to link compaction with depth, and for this we use the empirical stress vs. depth mapping function defined in Vernik (2016). The latter relies on a median stress-depth mapping function that ignores both lateral and vertical clay content variations in shale sections. Effective stress is calculated assuming hydrostatic pore pressure, and this workflow allows porosity normal compaction trends (NCTs) to be plotted in depth for a variety of shales and sandstones. Because shales typically comprise more than 75% of siliciclastic sequences, the same stress-depth mapping function can be assumed to analyze sands and sandstones with low clay content – the group of arenites.

Shale porosity

Yang and Aplin et al. (2004) fit a relationship between porosity (expressed as void ratio) and vertical effective stress in the process of shale compaction. These relationships provide a useful description of porosity reduction with depth, as they properly reflect the role of clay content in compaction. However, the relationships become non-physical at higher effective stresses (above 38MPa) where it can be observed that porosity erroneously decreases as a function of clay content. Alternatively, the simpler Rubey and Hubbert (1959) model possesses a form that preserves the increase in porosity with clay content at all depths. As shown by Vernik (2016), Rubey-Hubbert (RH) model should be preferred at depths greater than a few hundred meters, and also at shallower depths for significantly over-consolidated sediments. If the initial porosity in the RH model is also made clay content-dependent then these two models yield relatively similar results in the stress range from 5-30 MPa, i.e., where the shale normal compaction typically occurs.

Arenite porosity

Rigid grain-supported sands and sandstones with minor clay content (v_{cl} = 0.02-0.15), are referred to as arenites (Vernik, 2016). The porosity reduction with depth in these lithologies is more complex due to the mechanical compaction dominating at shallower depths being replaced by the chemical crystallization processes, such as quartz overgrowth development often referred to as quartz cementation.

Unlike the situation with shales, reliable models of mechanical compaction of sands do not exist, despite a great of petrographic data and core and calibrated log porosity measurements in shallow and deep wells (e.g., Lander and Walderhaug, 1999; Paxton et al., 2002). Paxton et al. (2002) consider the intergranular volume IGV as a main indicator of mechanical compaction in relatively clean sands, which essentially can be qualified as arenites and present an extensive data set of petrographic IGV data as a function of depth from provinces with limited uplift and erosion. An important quality of the IGV data is that these can be measured on cores from very deep wells with substantial cementation-induced porosity reduction. We use a power-law porosity reduction with stress that attempts to capture the Paxton et al. data set, that is controlled by the critical porosity at surface ϕ_c. However, the mechanical compaction must be complemented by the model that takes the chemical diagenesis (i.e., cementation) into account as well. The simple linear empirical model suggested by Ramm and Bjorlykke (1994) is employed beyond the consolidation porosity (ϕ_{con}). The latter separates the domains of unconsolidated and poorly consolidated arenites from more consolidated arenites, wherein further mechanical compaction is arrested to give rise to pervasive grain cementation (Vernik, 2016). The depth of the onset of pervasive cementation can range from 2000-2900 m depending on the geothermal gradient and/or pore fluid activity.

Bulk density NCT

Bulk density depth trends are needed in the construction of acoustic and shear impedance trends. We use the shale and arenite porosity in conjunction with a matrix density of 2.65g/cc for arenites and a variable matrix density for shales that increases with depth, as described in Vernik (2016).

Acoustic Impedance NCT

P- wave velocities are computed from the conventional shale rock physics model (RPM) of Vernik (2016), which uses a harmonic average of silt and clay grain moduli in combination with a power-law porosity dependence. We note that there is no explicit stress dependence in this model, but rather an implicit dependence through porosity, which makes it compatible with compactional pore pressure prediction models. S-wave velocity is calculated from the empirical Vp-Vs relation of Venik (2016) which accounts for a non-linear dependence at low velocities. Because the shale porosity NCT was computed using a normal pressure gradient and normal vertical effective stress (VESn), the *AI* and *SI* trends for shale are *de facto* their NCTs. For arenites we use the Vernik-

Kachanov RPM (Vernik, 2016), which is a combination of two independent models covering (1) the porosity ranges from 0 to the consolidation porosity (ϕ_{con}) and (2) from ϕ_{con} to the critical porosity of sand ϕ_c, which matches the chemical and mechanical diagenesis domains of porosity reduction.

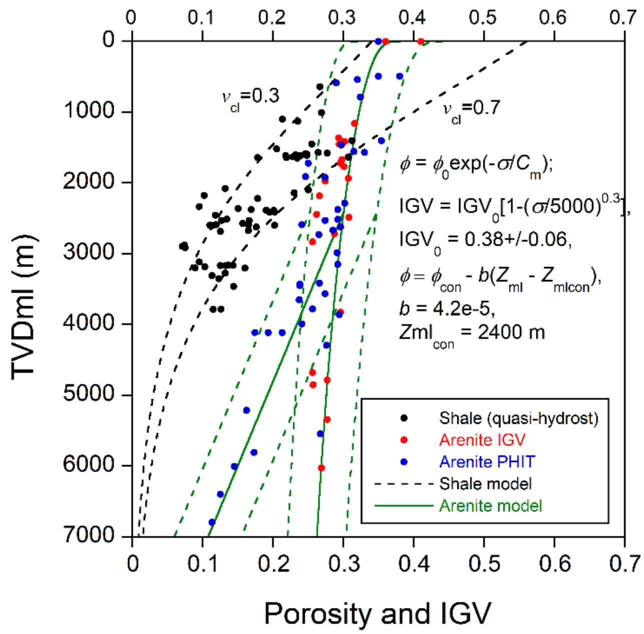

Figure 1: Porosity/IGV measurements vs. depth for normally compacted shales and variably pressured arenites (in the wider depth range). The consolidation depth is set to 2400 m.

To convert dry moduli to water-saturated moduli and velocities for arenites we use Gassmann's equation. For our realization of porosity modeling the critical porosity was 0.38±0.06, the consolidation porosity was set to 0.30±0.045, and the depth of consolidation was set at 2400 m.

Some of the results are shown in Figure 2, where the median AI trends are shown using the porosity NCT bounds for shale and arenites. Our data set of shale and arenite SI data (not shown) is equally matched by the models described, implying their robust performance

Conclusions

We have taken existing models of sediment compaction and combined them with rock physics models for velocities to arrive at guides for realistic elastic depth trends. Care has been taken to select high quality measurements for comparison to eliminate over-pressured and uplifted regimes that would obscure the underlying trends. We have achieved a good match, verifying the approach taken. We can also expand the domain of applicability through the use of fluid replacement modelling and pore pressure adjustment (for overpressure regimes) to create context-dependent depth trend bounds, which can then be used in seismic inversions studies.

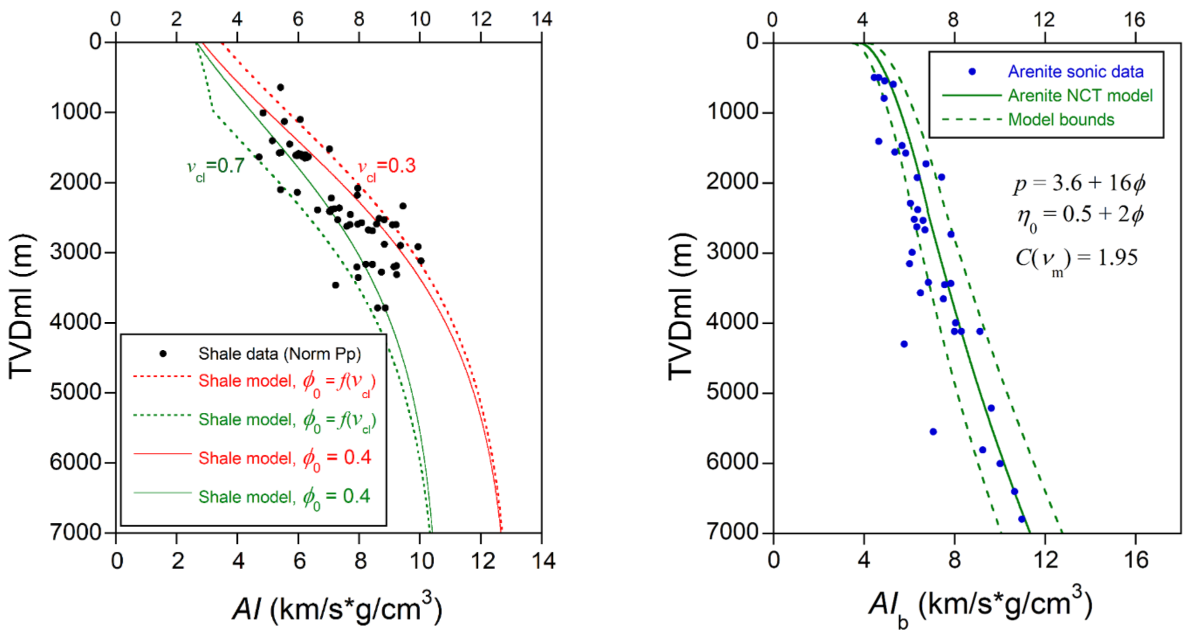

Figure 2: Acoustic impedance as a function of depth for shales (left) and arenites (right). NCT models are represented as lines while data points from various sources representing quasi-hydrostatic pore pressure intervals are also plotted. The data set was filtered to avoid areas of high geothermal gradient and/or uplifted/eroded terrains.

References

Athy L.F. 1930. Density, porosity and compaction of sedimentary rocks. American Association of Petroleum Geologists Bulletin, 31, 241–287.

Ramm M. and Byorlykke K. 1994. Porosity/depth trends in reservoir sandstones; assessing the quantitative effects of varying pore-pressure, temperature history and mineralogy, Norwegian Shelf data. Clay Minerals, 29, 475-490.

Issler, D.R. 1992. A new approach to shale compaction and stratigraphic restoration, Beaufort-Mackenzie basin and Mackenzie Corridor, Northern Canada, American Association of Petroleum Geologists Bulletin 76, (8), 1170-1189.

Lander R.H. and Walderhaug O. 1999. Predicting porosity through simulating sandstone compaction and quartz cementation. American Association of Petroleum Geologists Bulletin 83, (3), 443-449.

Paxton, S.T., Szabo, J.O., Ajdukiewicz, J. and Klimentdis, R.E. 2002. Construction of an intergranular volume compaction curve for evaluating and predicting compaction and porosity loss in rigid-grain sandstone reservoirs. American Association of Petroleum Geologists Bulletin 86, (12), 2047-2067.

Rubey W.W. and Hubbert M.K. 1959. Role of fluid pressure in mechanics of overthrust faulting II: Overthrust belt in geosynclinal area of western Wyoming in light of fluid-pressure hypothesis. Geological Society of America Bulletin, 70, (2) 167-206.

Vernik L. 2016. Seismic petrophysics in quantitative interpretation. Society of Exploration Geophysicists.

Yang Y. and Alpin A.C., 2004. Definition and practical application of mudstone porosity-effective stress relationships. Petroleum Geoscience 10, 153-162.